Glottal flow through a two-mass model

Vries, M.P. de; Schutte, H.K.; Veldman, Arthur; Verkerke, Gijsbertus

Glottal flow through a two-mass model: Comparison of Navier–Stokes solutions with simplified models

M. P. de Vries, H. K. Schutte, A. E. P. Veldman, and G. J. Verkerke

Artificial Organs, Biomedical Engineering, Ant. Deusinglaan 1, 9713 AV Groningen, The Netherlands

A new numerical model of the vocal folds is presented based on the well-known two-mass models of the vocal folds. The two-mass model is coupled to a model of glottal airflow based on the incompressible Navier–Stokes equations. Glottal waves are produced using different initial glottal gaps and different subglottal pressures. Fundamental frequency, glottal peak flow, and closed phase of the glottal waves have been compared with values known from the literature. The phonation threshold pressure was determined for different initial glottal gaps. The phonation threshold pressure obtained using the flow model with Navier–Stokes equations corresponds better to values determined in normal phonation than the phonation threshold pressure obtained using the flow model based on the Bernoulli equation. Using the Navier–Stokes equations, an increase of the subglottal pressure causes the fundamental frequency and the glottal peak flow to increase, whereas the fundamental frequency in the Bernoulli-based model does not change with increasing pressure. © *2002 Acoustical Society of America.* [DOI: 10.1121/1.1323716]

LIST OF SYMBOLS

CQ	closed quotient	k_1	lower spring stiffness
$\mathbf{F}$	vector representing external forces on the fluid	r_1	lower damper
F_0	fundamental frequency	m_2	upper mass
U_g	glottal peak flow	k_2	upper spring stiffness
p	pressure	r_2	upper damper
p_s	subglottal pressure	k_c	coupling stiffness
$\mathbf{u}$	vector with the velocity components	k_{col1}	lower collision spring stiffness
v	kinematic viscosity of the fluid	k_{col2}	upper collision spring stiffness
u	horizontal velocity of fluid	x_1	deflection of m_1
ν	vertical velocity of fluid	x_2	deflection of m_2
m_1	lower mass	ζ_1	lower damping ratio
		ζ_2	upper damping ratio

I. INTRODUCTION

To understand the process of voice production, several authors have investigated the pressure–flow relationship in the glottis (e.g., van der Berg *et al.*, 1957; Scherer and Titze, 1983; Alipour *et al.*, 1996, Guo and Scherer, 1993; Liljencrants, 1991). These examinations were all performed in a static glottis. Other investigations include the dynamic behavior of the voice source, which has been experimentally studied by Shadle *et al.* (1999) and Mongeau *et al.* (1997). Numerical modeling of the interaction between the oscillating vocal folds and the airflow in the glottis is performed using a simplified description of the vocal fold combined with a simplified description of the airflow (e.g., Ishizaka and Flanagan, 1972; Pelorson *et al.*, 1994; Story and Titze, 1995; Herzel *et al.*, 1995; Lous *et al.*, 1998). With these so-called lumped parameter models, glottal waves are produced as a result of a flow-induced oscillation of the vocal folds. Generally, in these lumped parameter models, the pressure and flow in the glottis are related by the Bernoulli equation. To apply this Bernoulli equation, assumptions concerning the physical characteristics of the fluid, air in our case, have to

be made. The use of the Bernoulli equation is allowed when the flow is assumed to be steady, laminar, nonviscous, and incompressible. In a cross section, pressure and velocity are usually assumed to be constant. In reality, pressure and velocity vary over a cross section. The velocity even has a transverse component that is ignored. Each of the assumptions, mentioned before, introduces an error and the resulting accumulation of errors results in an inaccurate description of the flow. To improve the flow calculations, a more accurate flow description has to be used. This is possible by using the two-dimensional Navier–Stokes equations. These equations describe the nonsteady and viscous behavior of a fluid under an external load. In this study, Navier–Stokes equations are implemented having only the assumption of incompressibility.

Although solving the Navier–Stokes equations is very time consuming, today's computing power ensures acceptable calculation times. Therefore, in the last decade, the Navier–Stokes equations already have been used in research concerning voice production. Alipour *et al.* (1996), Guo and Scherer (1993), and Liljencrants (1991) presented data using the Navier–Stokes equations in a static model of the vocal

folds. The pressure–flow relationships resulting from these investigations in the static glottis are related to the dynamic situation during phonation.

Recently, Alipour and Titze (1996) combined the incompressible Navier–Stokes equations with a dynamic finite-element method (FEM) model of the vocal folds and simulated phonation in this way. In their model, the finite-element method model of the vocal fold and the model of the Navier–Stokes equations exchange information, resulting in glottal waves. A disadvantage of this model is that it is only possible to prescribe a subglottal flow rate instead of an initial pressure. A preceding Bernoulli solution is needed in their model to approximate the flow rate that occurs at physiological subglottal pressures.

When the lumped parameter models of the vocal folds (Ishizaka and Flanagan, 1972; Herzel *et al.*, 1995; Pelorson *et al.*, 1994) are compared with the model of Alipour and Titze (1996), it can be seen that the glottal airflow description, based on the Bernoulli equation in the lumped parameter models, is replaced by the Navier–Stokes equations in the Alipour and Titze model, and the description of the vocal folds by a number of masses, springs, and dampers in the lumped parameter models is replaced by an FEM model. In the present study we will present a model composed of a lumped parameter model of the vocal folds combined with a Navier–Stokes model of the glottal flow. In this way, the need for assumptions concerning the viscous losses, as is needed in studies using a Bernoulli-based equation, is not necessary: as a consequence of the use of Navier–Stokes equations, viscous effects are included. We will give a comparison between results obtained using the Navier–Stokes equations with results obtained using the Bernoulli-based model. For the model of the vocal fold, we will use a lumped parameter model, i.e., the two-mass model. In this way, only one of the two steps presented by Alipour and Titze (1996) has been performed. This study is meant to be a step between the low-order models (the lumped parameter models) and the high-order models. Also, a new model of the aerodynamics is presented in which it is possible to prescribe the subglottal pressure.

II. MATERIALS AND METHODS

A model of one vibrating vocal fold has been developed, composed of a two-mass model describing the vocal fold and the Navier–Stokes equations describing the glottal flow. Due to symmetry, only one vocal fold is considered. First, the two-mass model simulating the vocal fold will be described, followed by the Navier–Stokes equations describing the aerodynamics. The interaction between the two-mass model and the Navier–Stokes equations will be described in a following section.

A. Two-mass model of the vocal folds

A two-mass model describes one vocal fold by two coupled oscillators (e.g., Ishizaka and Flanagan, 1972; Herzel *et al.*, 1995; Pelorson *et al.*, 1994; Lous *et al.*, 1998). Each oscillator consists of a mass, a spring, and a damper (Fig. 1). Mass m_1, spring stiffness k_1, and damper r_1 represent the lower part of the vocal fold. Mass m_2, spring stiff-
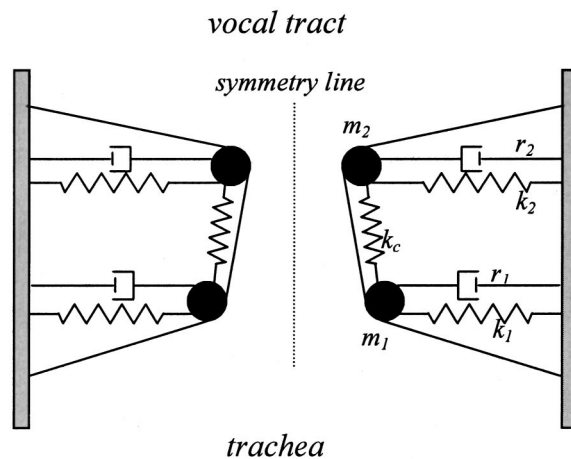

FIG. 1. Two-mass model.

ness k_2, and damper r_2 represent the upper part. The two masses are coupled by a spring with stiffness k_c. The two masses, m_1 and m_2, are permitted to move only in a lateral direction. The deflections of m_1 and m_2 are x_1 and x_2, respectively. In the two-mass model, symmetry with respect to a plane parallel to the main flow axis is assumed; therefore, only one vocal fold is considered. When the vocal fold approaches the symmetry line within a very short distance, collision springs with stiffness k_{col1} and k_{col2} are activated and have an influence on the masses m_1 and m_2, respectively, in the contralateral direction (e.g., Ishizaka and Flanagan, 1972; Pelorson *et al.*, 1994). In this way, the effective spring stiffness during collision changes. As a consequence of this way of modeling the collision, the glottal opening is allowed to have a small negative value.

In this study, we use two sets of values of the masses and springs. The first set of values consists of values used by Ishizaka and Flanagan (1972), which are also used by several other researchers (e.g., Herzel *et al.*, 1995; Steinecke and Herzel, 1995). The second set of values consists of values proposed by de Vries *et al.* (1999). This new set of parameters is based on a finite-element method (FEM) study of the mechanic behavior of a vocal fold. The values of the masses and springs are substantially smaller than the values used in previous studies. The parameter values for both sets are listed in Table I.

TABLE I. Parameter values for the two-mass model: Ishizaka and Flanagan parameters and de Vries parameters.

	I&F parameters	de Vries parameters
m_1 lower mass (g)	0.125	0.024
m_2 upper mass (g)	0.025	0.020
k_1 lower spring stiffness (N/m)	80	22
k_2 upper spring stiffness (N/m)	8	14
k_c coupling spring stiffness (N/m)	25	10
ζ_1 damping ratio (g/s)	0.1	
ζ_2 damping ratio (g/s)	0.6	
l_g glottal length (cm)	1.3	
k_{col1} collision spring stiffness (N/m)	$3k_1$	
k_{col2} collision spring stiffness (N/m)	$3k_2$	

B. Aerodynamics

To obtain oscillation of the vocal folds, aerodynamic forces have to act on the two masses. In the present study, the aerodynamic forces result from the pressure distribution along the glottal surface as determined by the Navier–Stokes equations. For the computation of the aerodynamic part of this model, the incompressible two-dimensional Navier–Stokes equations are used. These equations are based on two conservation laws.

(1) Conservation of mass

$$\nabla \cdot \mathbf{u} = 0, \tag{1}$$

where $\mathbf{u}$ is the vector with the velocity components.

(2) Conservation of momentum

$$\frac{\partial \mathbf{u}}{\partial t} + \nabla p = \mathbf{R}, \tag{2}$$

with

$$\mathbf{R} = -(\mathbf{u} \cdot \nabla)\mathbf{u} + \nu(\nabla \cdot \nabla)\mathbf{u} + \mathbf{F}.$$

In Eq. (2), p is the pressure, ν is the kinematic viscosity of the fluid, and F is the vector representing external forces on the fluid.

The term $\partial \mathbf{u}/\partial t$ in Eq. (2) is discretized in time with a forward Euler method using time step ∂t. This results in

$$\nabla \cdot \mathbf{u}^{n+1} = 0, \tag{3}$$

$$\frac{\mathbf{u}^{n+1} - \mathbf{u}^{n}}{\partial t} + \nabla p^{n+1} = \mathbf{R}^{n}, \tag{4}$$

where $n+1$ is the new time step and n is the present time step. These terms can be rearranged as

$$\mathbf{u}^{n+1} = \mathbf{u}^{n} + \partial t \mathbf{R}^{n} - \partial t \nabla p^{n+1}. \tag{5}$$

This can be substituted into Eq (3), which results in the Poisson equation for the pressure

$$(\nabla \cdot \nabla) p^{n+1} = \nabla \left(\frac{\mathbf{u}^{n}}{\partial t} + \mathbf{R}^{n} \right). \tag{6}$$

Spatial discretization of the Navier–Stokes equations is performed in a Cartesian grid. This grid can be refined at places of particular interest. The three degrees of freedom of each cell in the grid are the velocity in the direction of the main flow u, the velocity perpendicular to the main flow v, and the pressure p. The velocity in the direction of the main flow u is defined on the right edge of a cell, the velocity perpendicular to the main flow v is defined on the upper edge of a cell, and the pressure p is defined in the center of a cell. This staggered way of placing the variables is known as the marker-and-cell (MAC) method (Harlow and Welsh, 1965). The numerical advantage of this method is the uniqueness of the pressure.

The equations stated above have to be completed by boundary conditions. At the laryngeal wall, the tangential velocity is set to zero, simulating the sticking of the fluid to the wall, the so-called no-slip condition, and the perpendicular velocity is set to zero, simulating the impermeability of the wall. At the inlet, the subglottal pressure is prescribed.
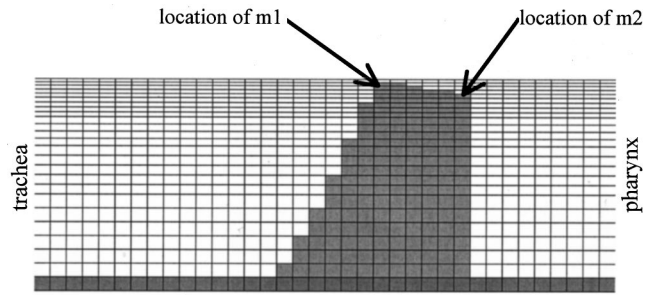

FIG. 2. Nonuniform grid with model of the vocal fold.

The outlet conditions combine a prescribed pressure with zero normal derivatives of the velocities. Since in the two-mass model only one vocal fold is modeled because of the symmetry assumption along the glottis, the aerodynamics is assumed to be symmetric along the glottis. At this symmetry line, the velocity perpendicular to the symmetry line is set to zero and the derivative of the axial velocity to its perpendicular coordinate is set also to zero.

The model of the aerodynamics makes use of adaptive time steps: within every time step, a routine checks for the time step to be small enough to give reliable results. The routine tries to calculate for the optimal time step for the present situation. This adaptive time step is profitable in the present research because the aerodynamic grid is changing during the simulation as a consequence of the moving vocal fold. In this way, a stable and fast solution is obtained. During the simulations presented in this study, the time step varied between 32.0E-6 and 0.5E-6 s. An exhaustive validation of an expanded version of the model of the aerodynamics is presented by Veldman et al. (1999).

To be able to compare the results using Navier–Stokes equations with results using simplified models, simulations with a glottal flow model based on Bernoulli are also used. The model used for comparison has been presented before by Lous et al. (1998).

C. Interaction

Interaction between the vocal fold and the aerodynamics takes place at the surface that is defined by the location of the two masses (Fig. 2). The masses are connected by rigid, massless plates. This configuration is also used by Lous et al. (1998), where they describe a two-mass model that uses the Bernoulli equation. In this configuration, sharp edges at the locations of the masses are present.

The interaction between the two-mass model and the aerodynamic model occurs in the grid of the aerodynamics. The cells of the grid in which a part of the two-mass model is present are supposed to be filled by a nonfluid material. In this way, a distinction is made between cells that are filled with air (aerodynamic cells) and cells that are not filled with air (mechanic cells). In the aerodynamic cells, the Navier–Stokes equations are calculated. The mechanic cells provide the boundary conditions for the aerodynamic cells. In the grid, information concerning the pressure of the airflow is transferred to the two-mass system, and information about

the position and the velocity of the two masses is transferred to the aerodynamic model in every time step.

The pressure distribution along the vocal-fold surface resulting from the Navier–Stokes calculations has to be translated to two point forces that act on the two masses. These forces are not directly available from the aerodynamic model, but are derived from the pressures in the aerodynamic cells adjacent to the vocal fold. The pressure values of the cells that contain air and that are also adjacent to the cells that contain a part of the vocal fold are multiplied by the area of the concerning cell, which corresponds to the length of the cell multiplied by the glottal length. These pressure forces are calculated in all fluid cells adjacent to the vocal-fold cells, so the complete glottal surface is considered. The pressure forces are distributed over the two masses in such a way that they form a statically equivalent system. The resulting new positions and velocities of the two masses are calculated and transferred to the aerodynamic model by defining a new distribution of aerodynamic cells and mechanic cells in the grid. The velocities of the mechanic cells at the glottal surface are calculated by interpolation of the velocities of the two masses. In this way, a dynamic boundary condition for the aerodynamic cells is defined, which is used in the next time step of the calculations of the Navier–Stokes equations. In this way, a realistic description of the interaction is obtained.

The two-mass model is by definition a two-dimensional model. Therefore, the aerodynamics is also considered to be two-dimensional. To obtain results as glottal flow and aerodynamic forces, the third dimension is simulated by assuming a uniform distribution of the aerodynamic quantities along the length of the vocal fold. According to measurements performed by Baer (1981), the length of the vocal fold is modeled by a length of 1.3 cm. In this way, boundary effects that occur at the anterior and posterior glottal commissure are neglected.

To determine the numerical validity of the model, the number of cells has been varied until a grid was obtained for which a doubling of the number of cells does not result in a noticeable difference in the glottal waves. The grid is made nonuniform by taking smaller cells in the neighborhood of the glottis, because in this region larger velocity gradients and pressure gradients can be expected.

To obtain glottal waves, different values for the subglottal pressure P_s were applied. In a previous study (de Vries *et al.*, 1999), the properties of glottal waves that are produced at a pressure of 6 cm H_2O were compared to normal values. We also used the value of 6 cm H_2O in this study, which is chosen after Holmberg *et al.* (1989), where they derived average values for several quantities concerning phonation in males and females. The normal value of the subglottal pressure of 4.3 cm H_2O, determined by Schutte (1980), has not been used because no glottal waves were obtained at that pressure for the specific set of model parameters used in our study. Properties of the glottal waves produced with the presented numerical model will be considered at $P_s = 0.6$ kPa, which is almost equal to 6 cm H_2O. In this

TABLE II. Properties of the glottal waves produced using the Navier–Stokes equations compared to normal values; these results were obtained using the de Vries parameters because the use of the Ishizaka and Flanagan parameters does not result in glottal waves.

| | Two-mass+ Bernoulli | Two-mass+ Navier-Stokes | Normal phonation | |
			Female	Male
Fundamental frequency F_0 (Hz)	187	165	207	119
glottal peak flow U_g(1/s)	0.25	0.48	0.14	0.23
closed quotient CQ(-)	0.30	0.30	0.26	0.39

way, properties of the glottal waves can be compared easily.

The glottal waves produced with the new model are analyzed and will be compared with the glottal waves produced by lumped parameter models using the Bernoulli-based model by comparing the fundamental frequency, glottal peak-flow rate, and closed quotient.

To obtain information about the phonation threshold pressure and the range of self-sustained oscillation, subglottal pressure was increased during the simulations by 8.0 kPa per second until a value of 2 kPa was reached. Simulations have been performed with an initial glottal gap of 0.0, 0.05, 0.01, and 0.25 mm. The initial shape of the glottis during these simulations was uniform, no diverging, and converging initial shapes are simulated.

III. RESULTS

Using a grid with 128×30 cells, the condition of stable solutions is satisfied. Therefore, this grid is used in all the simulations.

Using the parameters sets of Ishizaka and Flanagan and de Vries, different results were obtained. Using the Ishizaka and Flanagan parameter values, no self-sustained oscillation is obtained for subglottal pressures between 0.0 and 2.0 kPa and different initial glottal gaps. The de Vries parameters show self-sustained oscillation for a wide range of subglottal pressures and initial glottal gaps. Therefore, the following results are all produced using the de Vries parameters.

The properties of glottal waves resulting from a simulation with subglottal pressure of 0.6 kPa have been determined. Glottal waves with a closed phase could only be obtained using an initially closed glottis when a subglottal pressure of 0.6 kPa was applied. Comparisons of the properties of the glottal waves with the properties of the glottal waves produced using the Bernoulli-used model instead of the Navier–Stokes equations are summarized in Table II. For comparison, values for normal phonation according to Holmberg *et al.* (1989) are listed. From this table, it can be seen that the fundamental frequency appears to be lower by using the Navier–Stokes equations than by using the model based on the Bernoulli equation.

The glottal peak flow of the glottal waves produced using the Navier–Stokes equations is a factor of 2 higher than the glottal peak flow of the glottal waves produced using the Bernoulli-based model. This value is also higher than the
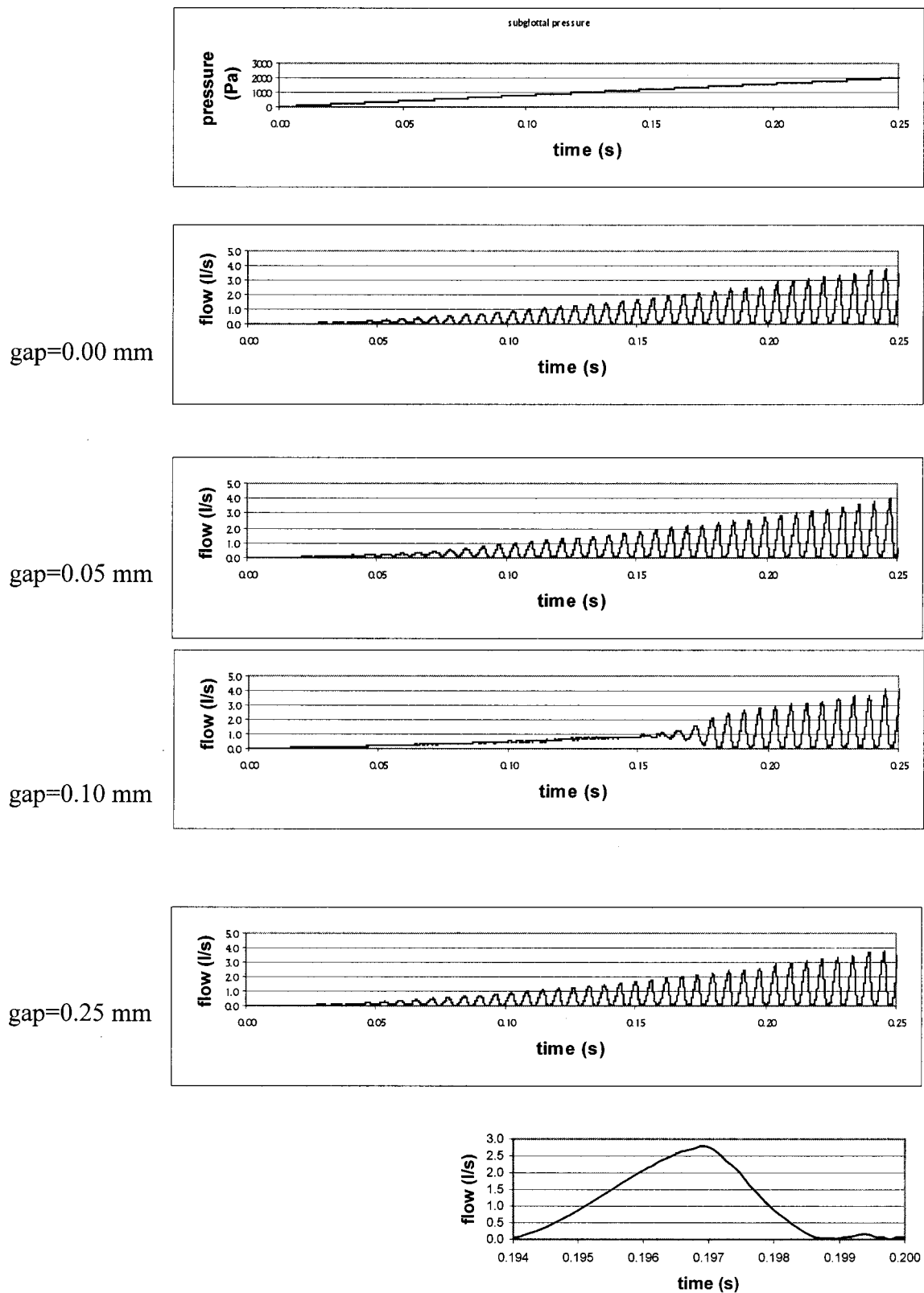
FIG. 3. Glottal waves for different initial glottal openings and rising subglottal pressure; at the bottom right, a close-up of one glottal wave (0.1-mm glottal gap) is shown.

normal value in female and male phonation, as shown in Table II.

Application of Navier–Stokes instead of the Bernoulli-based model does not influence the value of the closed quotient.

Results of an increase of subglottal pressure in the model using different values for the initial glottal gap are shown in Fig. 3. It can be seen that, using a different initial glottal gap, oscillation starts at a different subglottal pressure. The pressure at which self-sustained oscillation occurs
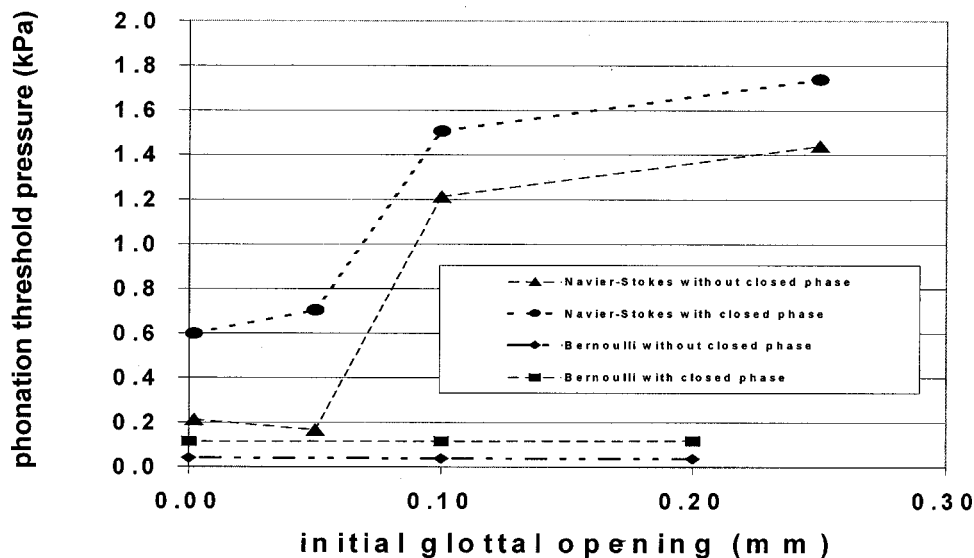
FIG. 4. Phonation threshold pressure for different initial glottal opening.

The graph legend reads:
- Navier–Stokes without closed phase
- Navier–Stokes with closed phase
- Bernoulli without closed phase
- Bernoulli with closed phase

(phonation threshold pressure) is shown in Fig. 4. At this phonation threshold pressure, a sinus-like waveform is obtained. Increasing the pressure above the phonation threshold pressure results in a more than proportional increase of the amplitude of the oscillation, resulting in glottal waves that are not sinus-like but which have a closed quotient. The pressure at which glottal waves with a closed quotient are obtained, is also plotted in Fig. 4. The phonation threshold pressure obtained is higher using the Navier–Stokes than when using the Bernoulli-based model (Fig. 4) for all initial glottal gaps. Titze (1988) studied the phonation threshold pressure for different initial glottal gaps; for a uniform glottis with an initial glottal gap of 0.1 mm, he determined a value of approximately 0.9 kPa, which is close to the value obtained using the Navier–Stokes equations of 1.2 kPa. The value obtained with the Bernoulli-based model is almost 0.1 kPa, which is much lower.

The rate of change of the fundamental frequency as a function of the subglottal pressure (dF_0/dP_s) is derived by dividing the difference between F_0 at 0.6 kPa ($F_0 = 165$ Hz) and at 1.6 kPa ($F_0 = 168$ Hz) by the difference in pressure (1.6 − 0.6 = 1.0 kPa). Over this pressure range, dF_0/dP_s is determined to be 3 Hz/kPa, which is almost equal to 0.3 Hz/cm H_2O. This value is substantially lower than the 2.5 Hz/cm H_2O determined by Ishizaka and Flanagan (1972) using their two-mass model. Using the glottal flow model that is based on the Bernoulli equation, the frequency remains unchanged when subglottal pressure is varied.

To demonstrate the variations in glottal flow during a glottal cycle, Fig. 5 shows the velocity component along the main flow direction in an open phase and in a closed phase, as determined during a simulation with the de Vries parameters with an initial glottal opening of 0.5 mm and a subglottal pressure of 0.8 kPa, resulting in a mean flow of 430 ml/s.

IV. DISCUSSION

In this study it is demonstrated that it is possible to achieve self-sustained oscillation with a two-mass model of the vocal folds in combination with a Navier–Stokes de-

scription of the glottal flow. The results show that the choice of the set of parameter values is crucial to achieve phonation: no self-sustained oscillation is obtained using the parameter values of Ishizaka and Flanagan (1972), while the use of the parameter values of de Vries et al. (1999) results in the production of acceptable glottal waves. This could be caused by the fact that the parameter values of Ishizaka and Flanagan are larger than those of de Vries. Probably the values of the masses and springs that represent the vocal folds are overestimated by Ishizaka and Flanagan, as suggested by Lous et al. (1998). In the case of an overestimation of the mechanic influence of the vocal folds, they predominate the dynamic behavior of the vocal folds.

The properties of the glottal waves produced using the Navier–Stokes equations differ from those produced using the Bernoulli-based model. Because applying the Navier–Stokes equations lowers the fundamental frequency, it can be
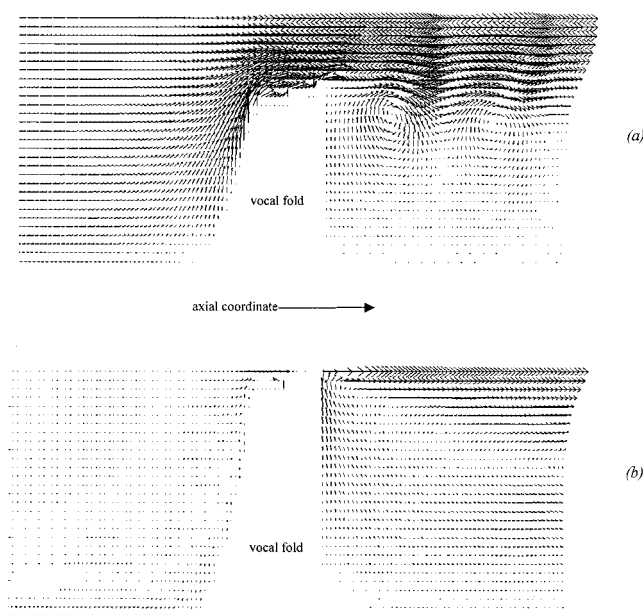

FIG. 5. Vector plot of velocities of maximum open phase (a) and closed phase (b).

1852   J. Acoust. Soc. Am., Vol. 111, No. 4, April 2002

de Vries *et al.*: Glottal flow   1852

stated that an increase in the effective mass of the vocal folds has been achieved. So, the lowering in the fundamental frequency might be partially explained by the influence of inertia effects which are present in the Navier–Stokes equation and absent in the Bernoulli equation. To which extent this effect contributes to the lowering is a question that will be answered in a forthcoming study.

The fact that the glottal peak flow is increased by a factor of 2 by applying the Navier–Stokes equations instead of the Bernoulli-based model can be explained by the fact that the viscous losses are described in a different manner: in the Bernoulli-based model, viscous effects are calculated using a fixed separation point for a convergent and divergent glottis. In the Navier–Stokes equations, the viscous effects in the main flow and in the boundary layer are described much more accurately, which can have a significant influence on the value of the glottal peak flow. The closed quotient of the glottal waves produced using the Navier–Stokes equations does not differ from the closed quotient produced using the Bernoulli-based model. The combination of a higher glottal peak flow with an equal closed quotient results in a higher glottal airflow velocity in the Navier–Stokes simulations than from the Bernoulli-based model. This also can be due to a different description of the viscous effects in both aerodynamic models.

The phonation threshold pressure depends on the initial glottal gap. This is in correspondence with Titze (1988), who stated that a tighter adduction of the vocal folds results in a lower phonation threshold pressure. The fact that a sinus-like oscillation occurs at a lower pressure using a gap of 0.05 mm can be explained by the fact that the initially closed glottis has to be opened first. The transition of a sinus-like oscillation to oscillation with a closed phase has also been demonstrated in normal phonation (Schutte and Seidner, 1988).

The value of the maximum jet velocity as shown in Fig. 5 corresponds very well with Alipour *et al.* (1996). In an excised larynx, they measured a supraglottal jet velocity of about 40 m/s at almost the same mean flow rate, namely 470 ml/s.

In the model presented in this paper, we are able to apply a subglottal pressure without using the Bernoulli equation to approximate the subglottal pressure for a given flow field, in contrast to Alipour and Titze (1996) and Guo *et al.* (1993). In comparison with Alipour and Titze (1996) we can state that, despite of our simple mechanical description of the vocal folds, we obtain glottal waves that are at least as realistic as in their study.

In our study, we assume the vocal folds to be sharp-edged because we do not apply any rounding to the geometry of the vocal fold. This choice is made because of the uncertain measures for rounding of the vocal folds that are available. Instead of the recommendations by Alipour and Titze (1999), no bulging of the vocal-fold surface is applied. If bulging is applied, the small pulses of air in the closed phase (which occur at higher pressure, as shown in Fig. 3) would probably be avoided. From this point of view, rounding of the vocal fold at the edges and bulging of the vocal-fold surface would be a possible improvement for the mechanical model.

Alipour, F., Scherer, R., and Knowles, J. (**1996**). ''Velocity distributions in glottal models,'' J. Voice **10**(1), 50–58.

Alipour, F., and Titze, I. R. (**1996**). ''Combined simulation of two-dimensional airflow and vocal fold vibration,'' in *Vocal Fold Physiology*, edited by P. J. Davis and N. H. Fletcher (Singular, San Diego), pp. 17–29.

Alipour, F., and Titze, I. R. (**1999**). ''Vocal fold bulging effects on phonation using biophysical computer model,'' NCVS Status Progress Report **13**, 105–114.

Baer, T. (**1981**). ''Observation on vocal fold vibration: Measurement of excised larynges,'' in *Vocal Fold Physiology*, edited by K. Stevens and M. Hirano (University of Tokyo, Japan), pp. 119–133.

de Vries, M. P., Schutte, H. K., and Verkerke, G. J. (**1999**). ''Determination of parameters for lumped parameter models of the vocal folds using a finite element method approach,'' J. Acoust. Soc. Am. **106**, 3620–3628.

Guo, C. G., and Scherer, R. C. (**1993**). ''Finite element simulation of glottal flow and pressure,'' J. Acoust. Soc. Am. **94**, 688–700.

Harlow, F. H., and Welsh, J. E. (**1965**). ''Numerical calculation of time-dependent viscous incompressible flow of fluid with free surface,'' Phys. Fluids **8**, 2182–2189.

Herzel, H., Berry, D., Titze, I. R., and Steinecke, I. (**1995**). ''Nonlinear dynamics of the voice: Signal analysis and biomechanical modelling,'' Chaos **5**(1), 30–34.

Holmberg, E. B., Hillman, R. E., and Perkell, J. S. (**1989**). ''Glottal airflow and transglottal air pressure measurements for male and female speakers in low, normal, and high pitch,'' J. Voice **3**(4), 294–305.

Ishizaka, K., and Flanagan, J. L. (**1972**). ''Synthesis of voiced sounds from a two-mass model of the vocal cords,'' Bell Syst. Tech. J. **51**, 1233–1267.

Liljencrants, I. (**1991**). ''Numerical simulations of glottal flow,'' in *Vocal Fold Physiology*, edited by J. Gauffin and B. Hammarberg (Raven, New York), pp. 99–104.

Lous, N. J. C., Hofmans, G. C. J., Veldhuis, R. N. J., and Hirschberg, A. (**1998**). ''A symmetrical two-mass vocal-fold model coupled to vocal tract and trachea, with application to prosthesis design,'' Acta Acust. (China) **84**(6), 1135–1150.

Mongeau, L., Franchek, N., Coker, C. H., and Kubli, R. A. (**1997**). ''Characteristics of a pulsating jet through a small modulated orifice, with application to voice production,'' J. Acoust. Soc. Am. **102**, 1121–1133.

Pelorson, X., Hirschberg, A., van Hassel, R. R., Wijnands, A. P. J., and Auregan, Y. (**1994**). ''Theoretical and experimental study of quasisteady-flow separation within the glottis during phonation. Application to a modified two-mass model,'' J. Acoust. Soc. Am. **96**, 3416–3431.

Scherer, R. C., and Titze, I. R. (**1983**). ''Pressure-flow relationships in a model of the laryngeal airway with a diverging glottis,'' in *Vocal Fold Physiology*, edited by P. J. Davis and N. H. Fletcher (Singular, San Diego), pp. 179–193.

Schutte, H. K. (**1980**). ''The efficiency of voice production,'' Ph.D. thesis, University of Groningen.

Schutte, H. K., and Seidner, W. W. (**1988**). ''Registerabhängige Differenzierung von Elektroglottogrammen. Sprache-Stimme-Gehör,'' **12**, 59–62.

Shadle, C. H., Barney, A., and Davies, P. O. A. L. (**1999**). ''Fluid flow in a dynamic mechanical model of the vocal folds and tract. Implications for speech production studies,'' J. Acoust. Soc. Am. **105**, 456–466.

Steinecke, I., and Herzel, H. (**1995**). ''Bifurcations in an asymmetric vocal-fold model,'' J. Acoust. Soc. Am. **97**, 1874–1884.

Story, B. H., and Titze, I. R. (**1995**). ''Voice simulation with a body-cover model of the vocal folds,'' J. Acoust. Soc. Am. **97**, 1249–1260.

Titze, I. R. (**1988**). ''The physics of small-amplitude oscillation of the vocal folds,'' J. Acoust. Soc. Am. **83**, 1536–1552.

van den Berg, J. W., Zantema, J. T., and Doornenbal, P. (**1957**). ''On the air resistance and the Bernoulli effect of the human larynx,'' J. Acoust. Soc. Am. **29**, 626–631.

Veldman, A. E. P., and Verstappen, R. W. C. P. (**1999**). ''Higher-order discretization methods for CFD,'' Nieuw archief voor de wiskunde **17**(2), 195–204.